liquids

MDPI

Article

Effect of Ligand Binding on Polymer Diffusiophoresis

Onofrio Annunziata

Department of Chemistry and Biochemistry, Texas Christian University, Fort Worth, TX 76129, USA; o.annunziata@tcu.edu; Tel.: +817-257-6215; Fax: +817-257-5851

Abstract: Diffusiophoresis is the migration of a macromolecule in response to a concentration gradient of a cosolute in liquids. Diffusiophoresis of polyethylene glycol (PEG) in water occurs from high to low concentration of trimethylamine-N-oxide (TMAO). This is consistent with the preferential hydration of PEG observed in the presence of TMAO. In other words, PEG migrates in the direction in which it lowers its chemical potential. On the other hand, although PEG is found to preferentially bind urea in water, PEG diffusiophoresis still occurs from high to low urea concentration. Thus, PEG migrates in the direction that increases its chemical potential in the urea case. Here, a ligand-binding model for polymer diffusiophoresis in the presence of a cosolute that preferentially binds to polymer is developed. It includes both actual polymer–ligand binding and the effect of the polymer on cosolute thermodynamic activity. This model shows that polymer–cosolute binding has a marginal effect on polymer diffusiophoresis and indicates that weak repulsive interactions, such as hard-core exclusion forces, are the main factor responsible for the observed PEG diffusiophoresis from high to low urea concentration. This work contributes to a better understanding of diffusiophoresis of macromolecules in response to gradients of nonelectrolytes.

Keywords: polyethylene glycol; urea; TMAO; preferential interaction; nonelectrolytes; osmolytes

Citation: Annunziata, O. Effect of Ligand Binding on Polymer Diffusiophoresis. *Liquids* **2023**, *3*, 414–425. https://doi.org/10.3390/liquids3040026

Academic Editor: Enrico Bodo

Received: 26 September 2023
Revised: 12 October 2023
Accepted: 16 October 2023
Published: 19 October 2023

1. Introduction

Macromolecules and colloidal particles in general are subject to diffusion-based transport in multi-component liquids relevant to a broad range of biochemical, biotechnological, geochemical, and industrial processes, such as centrifugation [1], dialysis [2], adsorption [3], crystallization [4], transport in microfluidics [5], living systems [6], gel media [7], insertion into dead-end pores [8], controlled release [9], and reaction kinetics [10,11]. Since concentration gradients of mixture components are usually present in these systems, diffusion coefficients are important for modeling the kinetic evolution of spatial concentration profiles within the liquid mixture.

A transport phenomenon known as diffusiophoresis has attracted much attention in recent years [12,13]. This is the isothermal and isobaric migration of a particle through a liquid in response to the directional concentration gradient of another solute (cosolute) present in the same liquid mixture. Although diffusiophoresis may occur in any liquid, this transport phenomenon is normally considered in the context of aqueous mixtures. Here, the solute responsible for diffusiophoresis of a colloidal particle is typically an inorganic salt or a low-molecular-weight water-soluble organic molecule [14,15].

Most studies have focused on diffusiophoresis of charged colloidal particles in the presence of salt gradients [16–20]. In this case, diffusiophoresis is caused by an electrophoretic mechanism that is ultimately related to the difference in mobility between the two salt ions in water (diffusion potential). However, it has been experimentally shown that diffusiophoresis is also observed for the macromolecule in polyethylene glycol (PEG) and PEG-based micelles [21–23]. This implies that gradients of salts or osmolytes can induce the migration of colloidal particles that are electrically neural.

PEG is a nonionic hydrophilic polymer found in many aqueous formulations relevant to pharmaceutical and biotechnological applications [24]. Furthermore, an important class

of water-soluble colloidal particles is represented by neutral particles whose interfacial properties are modified or governed by PEG. Indeed, this polymer has been employed for coating the surface of inorganic nanoparticles [25,26], proteins [27], micelles [28], and vesicles [29,30]. Since diffusiophoresis is mostly an interfacial phenomenon, understanding the diffusiophoresis of PEG coils is of fundamental importance for understanding the diffusiophoresis of PEG-based colloidal particles.

In previous studies, PEG diffusiophoresis has been connected to a thermodynamic phenomenon known as preferential hydration. This is described by the thermodynamic excess of water molecules near a macromolecule compared to bulk [31–33]. PEG is preferentially hydrated in the presence of osmolytes, such as trimethylamine-N-oxide (TMAO), and salts, such as NaCl and Na_2SO_4 [21–23,34]. Since PEG is preferentially hydrated in the presence of these cosolutes, diffusiophoresis occurs from a high to low cosolute concentration (positive diffusiophoresis) in order to lower PEG chemical potential.

Diffusiophoresis and preferential hydration can be examined within the framework of multicomponent diffusion [35,36]. Specifically, diffusion in a ternary aqueous system is characterized by a 2×2 diffusion coefficient matrix, in which one of the two cross-term diffusion coefficients relates to macromolecule diffusiophoresis due to the cosolute concentration gradient. The other cross-term, which is denoted as cosolute osmotic diffusion, describes cosolute diffusion due to a macromolecule concentration gradient and is closely related to preferential hydration [22]. Specifically, it has been shown that cosolute osmotic diffusion is important for determining water thermodynamic excess and, therefore, it characterizes the preferential hydration component of PEG diffusiophoresis [22,23].

The behavior of PEG diffusiophoresis was examined by considering a local domain model, in which cosolute concentration is depleted near the particle (local domain) compared to bulk fluid [22,31]. In the presence of particle diffusiophoresis, the local domain may be split into an inner local domain, in which fluid molecules move together with the particle, and an outer local domain, enclosing molecules moving with bulk fluid. It is only the outer domain that is responsible for diffusiophoresis. According to this model, a solute or solvent binding to a particle contributes to the inner fraction domain, whereas interactions that are weak compared to thermal energy or excluded-volume interactions [33,37,38] should contribute to the outer fraction domain. The fraction of the inner domain can be determined by combining diffusiophoresis and osmotic diffusion data.

There are also cosolutes that preferentially bind PEG: urea or thiocyanate salts [22,39]. In the presence of these cosolutes, water is depleted near PEG compared to bulk, leading to negative values of water thermodynamic excess. In this case, there is an expectation that diffusiophoresis occurs from a low to high cosolute concentration (negative diffusiophoresis) in order to lower PEG chemical potential. In contrast, it has been experimentally found that PEG diffusiophoresis remains positive even in the presence of such cosolutes [22,39]. In this paper, a model explaining the occurrence of positive diffusiophoresis even in the presence of a cosolute preferentially binding is developed. It specifically applies to the case of both the polymer and cosolute being electrically neutral and is suitable to describe PEG diffusiophoresis in the presence of urea.

2. Discussion

This section is organized into the following three subsections. In Section 2.1, the theoretical background on macromolecule diffusiophoresis and cosolute osmotic diffusion coefficients is outlined. These two transport coefficients are introduced within the framework of multicomponent-diffusion in ternary liquid mixtures. In Section 2.2, experimental data on PEG diffusiophoresis and cosolute osmotic diffusion in the presence of TMAO (preferential hydration) and urea (preferential binding) will be reviewed and interpreted by employing the local domain model. In Section 2.3, a novel ligand-binding model is developed in order to explain the positive diffusiophoresis of a polymer in the presence of cosolutes that preferentially bind to it.

2.1. Theoretical Background

For a ternary macromolecule(P)–cosolute(S)–solvent(W) system in isothermal and isobaric conditions and in the absence of convection, we can write the following [22]:

$$J_P = -D_{PP}\nabla C_P - D_{PS}\nabla C_S \tag{1a}$$

$$J_S = -D_{SP}\nabla C_P - D_{SS}\nabla C_S \tag{1b}$$

where J_P and J_S are the molar fluxes of macromolecule (P) and cosolute (S) in the solvent-fixed reference frame, respectively, C_P and C_S are the corresponding molar concentrations, and the four D_{ij}'s (with i,j = P,S) are multicomponent diffusion coefficients in the solvent-fixed reference frame. The main-term coefficients, D_{PP} and D_{SS}, describe the flux of the macromolecule and cosolute due to their own concentration gradients, while the cross-term coefficients, D_{PS} and D_{SP}, describe the flux of a solute due to the concentration gradient of the other solute. The cross-term, D_{PS}, corresponds to cosolute-induced macromolecule diffusiophoresis, while the other cross-term, D_{SP}, describes the cosolute osmotic diffusion due to the macromolecule concentration gradient.

In the limit of $C_P \to 0$, the diffusion rate of a macromolecule, $v_P = \lim_{CP\to 0}(J_P/C_P)$, is described by [40], as follows:

$$v_P = -D_P\left(\nabla \ln C_P + \hat{D}_{PS}\frac{\nabla \mu_S}{RT}\right) \tag{2}$$

where the second term in Equation (2) describes macromolecule diffusiophoresis while the first term is the Brownian diffusion rate caused by the entropic restoring force, with $D_P \equiv \lim_{CP\to 0} D_{PP}$ being the Brownian mobility (diffusion coefficient) of the macromolecule. In Equation (2), the unitless coefficient, $\hat{D}_{PS}$, is a reduced diffusiophoresis coefficient describing the effect of cosolute through the thermodynamic force, $-\nabla\mu_S$, where μ_S is the cosolute chemical potential, R the ideal gas constant and T the absolute temperature. We have the following [36]:

$$\frac{\nabla \mu_S}{RT} = \nu_S y_S \frac{\nabla C_S}{C_S} \tag{3}$$

where ν_S = 1 for non-electrolytes (e.g., urea or TMAO) and ν_S = 2 for symmetric electrolytes, and y_S is a known [22] thermodynamic factor characterizing the thermodynamic non-ideality of the binary cosolute–water system. Non-equilibrium thermodynamics can be then used to show that $\hat{D}_{PS}$ is connected to the cross-term, D_{PS} in Equation (1a), by [22,35], as follows:

$$\hat{D}_{PS} = \frac{1}{D_P}\frac{C_S}{\nu_S y_S}\lim_{C_P\to 0}\frac{D_{PS}}{C_P} \tag{4}$$

Non-equilibrium thermodynamics also show the following [22,35]:

$$\hat{D}_{PS} = \gamma - \lambda \tag{5}$$

where $\gamma \equiv \lim_{CP\to 0}(\partial\mu_P/\partial\mu_S)_{CP}$ is a thermodynamic preferential interaction coefficient, with μ_P being the macromolecule chemical potential. The other coefficient, λ, is a unitless Onsager transport coefficient defined by rewriting Equation (2) in the following way [21]:

$$v_P = -D_P\left(\frac{\nabla \mu_P}{RT} - \lambda\frac{\nabla \mu_S}{RT}\right) \tag{6}$$

Note that the negative sign preceding λ is a convention, chosen to ensure that this parameter assumes positive values in preferential hydration conditions.

Cosolute osmotic diffusion can be described by the ratio between the cross-term and main-term cosolute diffusion coefficient [35]. This is a unitless coefficient, $\hat{D}_{SP}$, given by the following [22]:

$$\hat{D}_{SP} \equiv \lim_{C_P \to 0} \frac{D_{SP}}{D_{SS}} = C_{SP} - \alpha\lambda \tag{7}$$

where $C_{SP} \equiv -\lim_{CP \to 0}(\partial C_S / \partial C_P)\mu_S$ is a cosolute partitioning coefficient [41] and $\alpha \equiv D_P/D_S$ is a macromolecule-to-cosolute mobility ratio, with D_S being the cosolute diffusion coefficient in the solvent-fixed reference frame, with $\alpha \approx 0.1$ or smaller. Since the $\alpha\lambda$ term in Equation (7) is small compared to the partitioning coefficient, C_{SP}, we have $\hat{D}_{SP} \approx C_{SP}$. This means that $\hat{D}_{SP}$ is approximately a thermodynamic quantity. The thermodynamic coefficient, γ, is linked to C_{SP} by [21], as follows:

$$C_{SP} = (1 - C_S\overline{V}_S)\gamma + C_S\widetilde{V}_P \tag{8}$$

where $\widetilde{V}_P \equiv \overline{V}_P - (\nu_S y_S)^{-1}\,\overline{V}_S$ with $\widetilde{V}_P$ and $\overline{V}_S$ being macromolecule and cosolute partial molar volumes, respectively. Note that $\overline{V}_P = \widetilde{V}_P$ is an excellent approximation because $\widetilde{V}_P >> \widetilde{V}_S$.

The coefficients, $\hat{D}_{PS}$ and $\hat{D}_{SP}$, are extracted from ternary diffusion coefficients using Equations (4) and (7) as a function of cosolute concentration, C_S. Although experimental values of $\hat{D}_{SP}(C_S)$ alone can be directly used to extract $\gamma(C_S)$ approximately, a combination of $\hat{D}_{PS}(C_S)$ and $\hat{D}_{SP}(C_S)$ data can be used to rigorously extract $\gamma(C_S)$ and $\gamma(C_S)$ from combination of Equations (5), (7) and (8).

As previously mentioned, water thermodynamic excess, ν_W, is introduced by employing the local domain model [22,31]. The following can be shown [21,42]:

$$\gamma = \nu_W \frac{C_S}{C_W} + \frac{\overline{V}_P - \widetilde{V}_P}{1 - C_S\overline{V}_S} C_S \cong \nu_W \overline{V}_W C_S \tag{9}$$

where $\widetilde{V}_W$ is water's partial molar volume. Thus, the value of ν_W is extracted by fitting the experimental data of $\gamma(C_S)$ to Equation (9). We then assume that the local domain is split into an inner local domain (I), in which fluid molecules move together with particle, and an outer local domain (II), enclosing molecules moving with bulk fluid. The thermodynamic excesses in the inner and outer domain are ${\nu_W}^{(I)}$ and ${\nu_W}^{(II)}$, respectively; with $\nu_W = {\nu_W}^{(I)} + {\nu_W}^{(II)}$ [22]. According to this model, the ratios, λ/γ and $\hat{D}_{PS}/\gamma$, are constants representing the two complementary fraction of inner and outer domain, respectively. We have the following:

$$\frac{\lambda}{\gamma} = \frac{\nu_W^{(I)}}{\nu_W^{(I)} + \nu_W^{(II)}} \tag{10a}$$

$$\frac{\hat{D}_{PS}}{\gamma} = \frac{\nu_W^{(II)}}{\nu_W^{(I)} + \nu_W^{(II)}} \tag{10b}$$

Thus, the values of ${\nu_W}^{(I)}$ and ${\nu_W}^{(II)}$ can be extracted from the experimental data of ν_W and $\hat{D}_{PS}/\gamma$.

2.2. Analysis of Experimental Data

In this section, the $\hat{D}_{PS}(C_S)$ and $\hat{D}_{SP}(C_S)$ data [22] on aqueous PEG (nominal molecular weight, 20 kg/mol) in the presence of TMAO and urea at 25 °C will be reviewed. These data will be then used to extract the corresponding values of ${\nu_W}^{(I)}$ and ${\nu_W}^{(II)}$.

It is convenient to examine cosolute osmotic diffusion prior to PEG diffusiophoresis due to its more direct connection to the thermodynamic quantity, γ. In Figure 1, cosolute osmotic diffusion coefficient, $\hat{D}_{SP}$, as a function of osmolyte concentration, C_S, is shown. As we can see, $\hat{D}_{SP}$ data are positive for both cosolutes, thereby implying that the cosolute diffuses from high to low PEG concentration. We can also see that $\hat{D}_{SP}$ lin-

early increases with C_S starting from $\hat{D}_{SP}$ (0) = 0. This behavior is in agreement with $\hat{D}_{SP} \approx C_{SP} = (\overline{V}_P + \nu_W \overline{V}_W)C_S$ based on Equations (8) and (9), with $\overline{V}_W = 18.07$ cm^3·mol^{-1}. For comparison, the reference line, $\overline{V}_P C_S$ (with $\overline{V}_P = 16.7$ dm^3·mol^{-1}) is included in the same figure. Positive deviations from this line correspond to positive values of water thermodynamic excess, ν_W. We can then deduce that PEG is preferentially hydrated in the presence of TMAO. Indeed, the application of Equations (5), (7) and (8) to $\hat{D}_{PS}(C_S)$ and $\hat{D}_{SP}(C_S)$ data, which confirms that $\hat{D}_{SP} \approx C_{SP}$ is a good approximation, rigorously yields $\gamma(C_S)$. We can then determine the thermodynamic excess of water molecules [43] near PEG using Equation (9), which is $\nu_W = 2600$ (5.7 per ethoxy group) in the TMAO case. In contrast, urea is preferentially binding to PEG because $\hat{D}_{SP}$ data lay below the reference line. In this case, the water thermodynamic excess is $\nu_W = -580$ (-1.3 per ethoxy group). It is interesting to observe that the effect of TMAO and urea on PEG follows the same behaviour observed in the case of proteins.

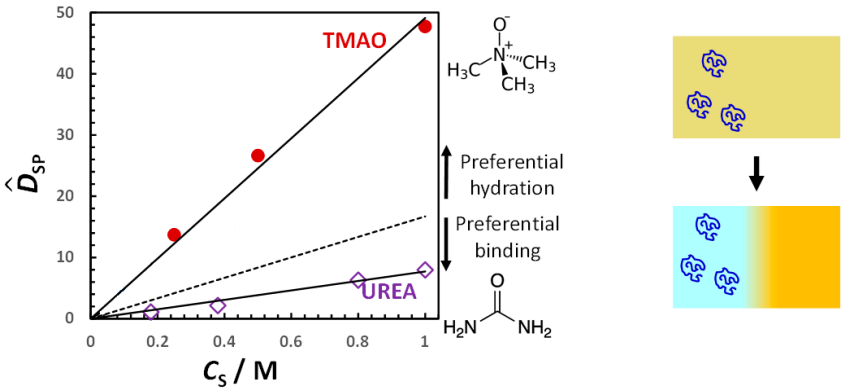

Figure 1. Cosolute osmotic diffusion coefficient, $\hat{D}_{SP}$, as a function of cosolute concentration, C_S, in the TMAO and urea cases. Dashed line represents $\overline{V}_P C_S$. Graphic representation on the right describes cosolute osmotic diffusion occurring from high to low concentration of PEG coils. Data taken from Ref. [22].

In Figure 2, the PEG diffusiophoresis coefficient, $\hat{D}_{PS}$, as a function of cosolute concentration, C_S, is shown. As we can see, $\hat{D}_{PS}$ data are also positive, thereby implying that PEG diffusiophoresis occurs from a high to low osmolyte concentration in both cases. Moreover, as in the case of osmotic diffusion data, $\hat{D}_{PS}$ linearly increases with C_S starting from $\hat{D}_{PS}(0) = 0$. The slope trend of diffusiophoresis data is the same as that of osmotic diffusion data in Figure 1, with PEG diffusiophoresis being larger in the TMAO case. In the urea case, although PEG prefers to interact more with urea than water, PEG diffusiophoresis still occurs from the high to low urea concentration.

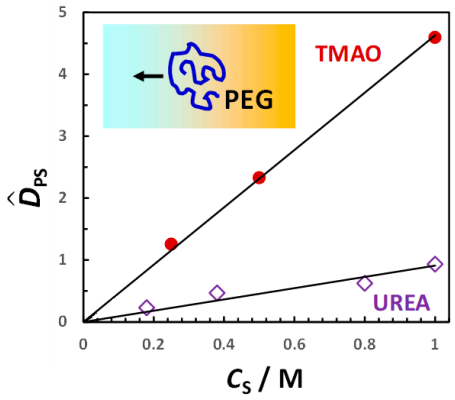

Figure 2. PEG diffusiophoresis coefficient, $\hat{D}_{PS}$, as a function of cosolute concentration, C_S, in the TMAO and urea cases. Inset is a graphic representation of PEG diffusiophoresis occurring from high to low cosolute concentration. Data taken from Ref. [22].

Since both $\hat{D}_{PS}$ and γ are directly proportional to C_S, the ratio, $\hat{D}_{PS}/\gamma$, is a constant, consistent with the local domain model. In the TMAO case, we have $\hat{D}_{PS}/\gamma = 0.14$, which gives ${\nu_W}^{(I)} = +2200$ (4.8 per ethoxy group) in the inner domain and ${\nu_W}^{(II)} = +360$ (0.80 per ethoxy group) in the outer domain. This result is consistent with a weakening of PEG preferential hydration as we move from the inner to the outer domain. In the urea case, the negative value of $\hat{D}_{PS}/\gamma = -0.10$ is the result of $\hat{D}_{PS}$ being positive and γ being negative (due to urea preferential binding, $\nu_W = -580$). This leads to ${\nu_W}^{(I)} = -640$ (-1.4 per ethoxy group) for the inner domain but ${\nu_W}^{(II)} = +60$ (0.13 per ethoxy group) for the outer domain. The negative value of ${\nu_W}^{(I)}$ is attributed to an actual PEG–urea binding process in the inner domain. However, a simple weakening of PEG–urea binding interaction should yield a negative value of ${\nu_W}^{(II)}$ in the outer domain too. Thus, the observed sign inversion of water thermodynamic excess is inconsistent with an actual physical division into inner and outer spatial domains. We should, therefore, generalize the actual definition of inner and outer domains as just two categories separating strong binding interactions from non-binding interactions, independent of spatial location. For example, excluded volume interactions invariably start at the macromolecule surface, but they should be formally attributed to the outer domain [33,37,38]. We can, therefore, explain PEG diffusiophoresis in the urea case by considering that the overall PEG–urea interactions are the result of an actual PEG–urea binding process (inner domain, ${\nu_W}^{(I)} < 0$) and residual excluded volume interactions, which are associated with the outer domain and are responsible for ${\nu_W}^{(II)} > 0$. A ligand-binding model supporting this conclusion is developed in Section 2.3.

2.3. Ligand-Binding Model for Polymer Diffusiophoresis

In this section, the mathematical expressions of γ and $\hat{D}_{PS}$ are derived by considering both polymer–ligand-binding and non-binding interactions. It will be shown that this model is consistent with experimental results on PEG diffusiophoresis in the presence of urea.

We start by assuming that there is a reversible binding of cosolute ligand S on the linear chain of a polymer, P, according to the following:

$$PS_{i-1} + S \rightleftharpoons PS_i \text{ with } i = 1, 2, \ldots, n$$

with n being the total number of sites on the polymer chain. This binding process is characterized by the chemical equilibrium condition as follows:

$$K_i = \frac{[PS_{i-1}]}{[PS_i]}\, a_S \tag{11}$$

where a_S is the thermodynamic activity of cosolute, S. Note that the activity coefficient of the PS_{i-1} complex is assumed to be the same as that of the PS_i complex. In this way, the ratio of their activities is the same as that of their concentrations, $[PS_{i-1}]/[PS_i]$. Even if these activity coefficients are not assumed to be equal to each other, they will approach one when taking the limit of $C_P \to 0$, consistent with the application of Equation (2). We then assume that the thermodynamic activity of cosolute can be written as follows:

$$a_S = f_S \cdot [S]' \tag{12}$$

where

$$[S]' = \frac{[S]}{1 - \varepsilon\, \overline{V}_P C_P + \ldots} \tag{13}$$

with [S] being the molar concentration of free cosolute in the polymer–cosolute–water mixture. The cosolute concentration, [S]′, describes the effect of C_P on cosolute thermodynamic activity. It represents the concentration of free S in a binary cosolute–water reservoir that is in chemical equilibrium with the ternary polymer–cosolute–water mixture through a membrane that is not permeable to polymer. In Equation (13), ε is a unitless interaction

coefficient characterizing the effect of polymer on [S]′ to the first-order with respect to C_P. If ε is positive, then [S]′ is larger than [S]. This situation describes the excluded volume effect of the polymer chain exerted on cosolute. Higher-order terms in the denominator of Equation (13) are not included because they vanish in the limit of $C_P \to 0$. In Equation (12), f_S is the activity coefficient of L. It is assumed to be the same as that of the binary cosolute–water reservoir. This implies that f_S is a function of [S]′. The thermodynamic non-ideality factor, y_S in Equation (2), is then given by the following:

$$y_S = 1 + \frac{d \ln f_S}{d \ln [S]'} \tag{14}$$

The cosolute partitioning coefficient, C_{SP}, can written as follows:

$$C_{SP} = -\lim_{C_P \to 0} \left(\frac{\partial C_S}{\partial C_P} \right)_{a_S} = \lim_{C_P \to 0} \frac{(\partial \ln a_S / \partial C_P)_{C_S}}{(\partial \ln a_S / \partial C_S)_{C_P}} \tag{15}$$

The partial derivatives of $\ln a_S$ in the numerator and denominator of Equation (15) are given by the following:

$$\left(\frac{\partial \ln a_S}{\partial C_S} \right)_{C_P} = \left(\frac{\partial \ln [S]}{\partial C_S} \right)_{C_P} + \frac{d \ln f_S}{d \ln [S]'} \left(\frac{\partial \ln [S]'}{\partial C_S} \right)_{C_P} = y_S \left(\frac{\partial \ln [S]}{\partial C_S} \right)_{C_P} \tag{16a}$$

$$\left(\frac{\partial \ln a_S}{\partial C_P} \right)_{C_S} = \left(\frac{\partial \ln [S]}{\partial C_P} \right)_{C_S} + \frac{d \ln f_S}{d \ln [S]'} \left(\frac{\partial \ln [S]'}{\partial C_P} \right)_{C_S} + \varepsilon \overline{V}_P = y_S \left[\varepsilon \overline{V}_P - \left(\frac{\partial \ln [S]}{\partial C_S} \right)_{C_P} \left(\frac{\partial C_S}{\partial C_P} \right)_{[S]} \right] \tag{16b}$$

where we have used Equation (13) to deduce the following:

$$\left(\frac{\partial \ln [S]'}{\partial C_S} \right)_{C_P} = \left(\frac{\partial \ln [S]'}{\partial \ln [S]} \right)_{C_P} \left(\frac{\partial \ln [S]}{\partial C_S} \right)_{C_P} = \frac{1}{[S]} \left(\frac{\partial [S]}{\partial C_S} \right)_{C_P} \tag{17a}$$

$$\left(\frac{\partial \ln [S]'}{\partial C_P} \right)_{C_S} = \left(\frac{\partial \ln [S]'}{\partial \ln [S]} \right)_{C_P} \left(\frac{\partial \ln [S]}{\partial C_P} \right)_{C_S} + \left(\frac{\partial \ln [S]'}{\partial C_P} \right)_{[S]} = -\frac{1}{[S]} \left(\frac{\partial [S]}{\partial C_S} \right)_{C_P} \left(\frac{\partial C_S}{\partial C_P} \right)_{[S]} + \varepsilon \overline{V}_P \tag{17b}$$

After substituting Equations (16a) and (16b) into Equation (15), we have the following:

$$C_{SP} = \lim_{C_P \to 0} \left[\left(\frac{\partial C_S}{\partial [S]} \right)_{C_P} \varepsilon \overline{V}_P [S] - \left(\frac{\partial C_S}{\partial C_P} \right)_{[S]} \right] \tag{18}$$

Note that C_{SP} does not depend on the non-ideality thermodynamic factor, y_S. To determine $C_S([S], C_P)$, we consider the mass balances for P and S as follows:

$$C_P = [P] + \sum_{i=1}^{n} [PS_i] = [P] \left(1 + \sum_{i=1}^{n} \beta_i {a_S}^i \right) \tag{19a}$$

$$C_S = [S] + \sum_{i=1}^{n} i [PS_i] = [S] + [P] \sum_{i=1}^{n} \beta_i i \, {a_S}^i \tag{19b}$$

where we have also used Equation (11) and introduced the cumulative associative constant $\beta_i \equiv \prod_{j=1}^{i} (K_j)^{-1}$ so that $[PS_i] = \beta_i [P] \, {a_S}^i$. We can remove polymer free concentration, [P], from Equation (18b) by combining the two mass balances in the following way:

$$C_S = [S] + C_P \frac{\sum_{i=1}^{n} \beta_i i \, {a_S}^i}{1 + \sum_{i=1}^{n} \beta_i \, {a_S}^i} \tag{20}$$

We are now in a position to differentiate C_S with respect to [S] and C_P. This yields the following:

$$\left(\frac{\partial C_S}{\partial [S]}\right)_{C_P} = 1 + C_P(< i^2 > - < i >^2)\left(\frac{\partial \ln a_S}{\partial [S]}\right)_{C_P} \quad (21a)$$

$$\left(\frac{\partial C_S}{\partial C_P}\right)_{[S]} = < i > + C_P(< i^2 > - < i >^2)\left(\frac{\partial \ln a_S}{\partial C_P}\right)_{[S]} \quad (21b)$$

where we have introduced the mean degree of cosolute binding, as follows:

$$< i^j > \equiv \frac{\sum_{i=0}^{n} i^j [PS_i]}{\sum_{i=0}^{n} [PS_i]} = \frac{\sum_{i=0}^{n} i^j [PS_i]}{C_P} \quad (22)$$

Note that $< i > = \sum_{i=0}^{n} i\ [PS_i]/C_P$ (case of $j = 1$) in Equation (21b) represents the average number of cosolute molecules bound to a polymer chain, while the factor, $< i^2 > - < i >^2$, in Equations (21a) and (21b) represents the variance of the number of cosolute molecules bound to a polymer chain. Since the terms containing the variance factor in Equations (21a) and (21b) are directly proportional to C_P, they can be neglected in the limit of $C_P \to 0$. Thus, substitution of $(\partial C_S/\partial [S])_{C_P} = 1$ and $(\partial C_S/\partial C_P)_{[S]} = < i >_0$ into Equation (18), with $<i>_0 \equiv \lim_{CP \to 0} <i>$, finally yields:

$$C_{SP} = \varepsilon\, \overline{V}_P C_S - < i >_0 \quad (23)$$

where we have also used $C_S = \lim_{CP \to 0}[S]$. To appreciate the dependence of $<i>_0$ on C_S, we can consider the special case of identical and independent binding sites, [44] which corresponds to $\beta_i \equiv \binom{n}{i} K^{-i}$ in Equation (20), with K being the intrinsic equilibrium dissociation constant of a site. In this case, the average number of cosolute molecules bound to a polymer chain is $<i>_0 = nC_S/(K + C_S)$. Due to cosolute binding, $<i>_0$ is directly proportional to C_S at low cosolute concentration and approaches the value of the total number of sites, $n = \lim_{CS \to \infty} <i>_0$ at a high cosolute concentration.

To obtain the expression of $\hat{D}_{PS}$, we need to derive the expression of γ from C_{SP}. Accordingly, we use Equation (8) to write the following:

$$\gamma = \frac{\Omega\, C_S - < i >_0}{1 - C_S \overline{V}_S} \quad (24)$$

where $\Omega \equiv \varepsilon\, \overline{V}_P - \widetilde{V}_P$. This volumetric coefficient is positive in the presence of excluded-volume interactions as it will be discussed below. Note that $1 - C_S\overline{V}_S \approx 1$ because $C_S\overline{V}_S$ represents a relatively small volume fraction in the experimental urea concentration range shown in Figures 1 and 2. If we also assume that $<i>_0 = (n/K)\ C_S$ (with $K >> C_S$), Equation (24) reduces as follows:

$$\gamma = \left(\Omega - \frac{n}{K}\right) C_S \quad (25)$$

We now turn our attention to the transport coefficients, λ, introduced by Equation (6). We introduce a simple diffusion law for each PS_i complex in a dilute solution of polymer, as follows:

$$-J_i = \frac{[PS_i]\, D_{PS_i}}{RT} \nabla \mu_i \text{ with } i = 0, 1, 2, \ldots, n \quad (26)$$

where J_i, D_{PS_i}, and μ_i are the molar flux, tracer diffusion coefficient, and chemical potential of the PS_i complex i, respectively. Note that diffusion of the free polymer is described by the case of $i = 0$. The expressions of total fluxes of polymer (J_P) and cosolute (J_S) follow the mass balances given by Equations (19a) and (19b). We, therefore, have the following:

$$J_P = \sum_{i=0}^{n} J_{PS_i} = -\sum_{i=0}^{n} [PS_i] D_{PS_i} \frac{\nabla \mu_{PS_i}}{RT} \quad (27a)$$

$$J_S = J_{[S]} + \sum_{i=1}^{n} i\, J_{PS_i} = J_{[S]} - \sum_{i=0}^{n} i\, [PS_i] D_{PS_i} \frac{\nabla \mu_{PS_i}}{RT} \tag{27b}$$

where $J_{[S]}$ is the molar flux of free cosolute. We assume that polymer–cosolute reversible binding is fast compared to diffusion. This implies that we can locally apply the chemical equilibrium condition as follows:

$$\nabla \mu_{PS_i} = \nabla \mu_P + i\, \nabla \mu_S \tag{28}$$

Substitution of Equation (28) into Equations (27a) and (27b) yields the following:

$$J_P = -C_P D_P^{(0)} \frac{\nabla \mu_P}{RT} - C_P < i > D_P^{(1)} \frac{\nabla \mu_S}{RT} \tag{29a}$$

$$J_S = J_{[S]} - C_P < i^2 > D_P^{(2)} \frac{\nabla \mu_S}{RT} - C_P \ < i > D_P^{(1)} \frac{\nabla \mu_P}{RT} \tag{29b}$$

where we have introduced the mean diffusion coefficient, as follows:

$$D_P^{(j)} \equiv \frac{\sum_{i=0}^{n} i^j\, [PS_i]\, D_{PL_i}}{\sum_{i=0}^{n} i^j\, [PS_i]} \tag{30}$$

with $D_P^{(0)}$ being the same as D_P in Equation (1). Note that the coefficient multiplying $\nabla \mu_S$ in Equation (29a) is equal to the coefficient multiplying $\nabla \mu_P$ in Equation (29b). This equality represents the Onsager reciprocal relation [45,46]. To determine λ, we can directly compare Equation (29a) to Equation (6), remembering that $v_P = \lim_{CP \to 0} (J_P / C_P)$. This finally yields the following:

$$\lambda = -\frac{D_P^{(1)}}{D_P^{(0)}} < i >_0 \tag{31}$$

Substitution of Equation (24) for γ and Equation (31) for λ into Equation (5) yields the following:

$$\hat{D}_{PS} = \frac{\Omega\, C_S - < i >_0}{1 - C_S \overline{V}_S} + \frac{D_P^{(1)}}{D_P^{(0)}} < i >_0 \tag{32}$$

We are now going to discuss the behavior of $\hat{D}_{PS}(C_S)$ based on Equation (32). As in the case of γ, we shall assume that $C_S \overline{V}_S << 1$ in Equation (32). This leads to the following:

$$\hat{D}_{PS} = \Omega\, C_S + \left(\frac{D_P^{(1)}}{D_P^{(0)}} - 1 \right) < i >_0 \tag{33}$$

The term proportional to $<i>_0$ in Equation (33) characterizes the effect of polymer–cosolute binding on polymer diffusiophoresis. It is expected that polymer–ligand association causes the size of PS_i to increase with the number of bound S molecules, i. This implies that the diffusion coefficient, D_{PS_i}, decreases as i increases. We also know that the first-order mean diffusion coefficient, $D_P^{(1)}$, weighs more than the zero-order mean diffusion coefficient, $D_P^{(0)}$, a higher molecular weight species (see Equation (30)). We, therefore, conclude that $D_P^{(1)} < D_P^{(0)}$. Thus, the second term in Equation (33) is negative and is predicted to drive polymer diffusiophoresis from a low to high cosolute concentration. This result is consistent with previously reported 1:1 host–guest diffusion models in which the diffusion coefficient of the host–guest complex is lower than that of free host and guest molecules [47,48]. However, in the case of polymers, it is reasonable to assume that binding of small cosolute molecules does not significantly affect the size of the polymer. In this case, D_{PL_i} is approximately independent of i and $D_P^{(1)} / D_P^{(0)} \approx 1$. This implies that the

second term in Equation (33) is expected to be small. If we then assume that $D_P^{(1)}/D_P^{(0)} = 1$, Equation (33) reduces to the following:

$$\hat{D}_{PS} = \Omega\, C_S \tag{34}$$

This result shows that, essentially, a cosolute binding to a polymer has no effect on polymer diffusiophoresis. Indeed, only the non-binding interactions are responsible for diffusiophoresis, consistent with the local domain model discussed in Section 2. We can then use Equation (34) for $\hat{D}_{PS}$ and Equation (25) for γ to write the following:

$$\frac{\hat{D}_{PS}}{\gamma} = \frac{\Omega}{\Omega - (n/K)} \tag{35}$$

We are now in position to compare Equation (35) with Equation (10b) for the local domain model, bearing in mind that $\gamma = (n_W{}^{(I)} + n_W{}^{(II)})\overline{V}_W C_S$. We deduce the following:

$$\nu_W^{(I)}\overline{V}_W = -\frac{n}{K} \tag{36a}$$

$$\nu_W^{(II)}\overline{V}_W = \Omega \tag{36b}$$

These equations can be used to describe experimental results on the PEG–urea–water system. The experimental value of $n_W{}^{(I)} = -640$ for the inner domain characterizes polymer-ligand actual binding. We can use this value to deduce that $K/n = 0.086$ M. For PEG with a molecular weight of 20 kg·mol^{-1}, there are 454 monomers. If each monomer is assumed to be a binding site, we calculate that $K = 39$ M. This value, which characterizes a weak polymer–cosolute physical binding, is consistent with the approximation $\langle i \rangle_0 = nC_S/(K + C_S) \approx (n/K)C_S$ within the experimental urea concentration range ($K >> C_S$). The experimental value of $n_W{}^{(II)} = 60$ for the outer domain corresponds to a positive value of the interaction term, $\Omega(\Omega/\overline{V}_P = 0.065)$ and can be attributed to repulsive excluded volume interactions. According to the Kirkwood–Buff theory, repulsive hard-core exclusion forces are described by the following equation [33]:

$$\Omega = V_{P,S}^{(ex)} - V_{P,W}^{(ex)} \tag{37}$$

where $V_{P,S}^{(ex)}$ and $V_{P,W}^{(ex)}$ are the volumes excluded to the center of cosolute and solvent molecule due to the presence of polymer, respectively. Because urea ($\overline{V}_S = 44$ cm^3·mol^{-1}) is larger than water ($\overline{V}_W = 18$ cm^3·mol^{-1}), [22] the excluded volume for urea is expected to be larger than that for water, making Ω a positive quantity, consistent with experimental findings. According to this analysis, PEG diffusiophoresis from a high to low urea concentration is driven by $V_{P,S}^{(ex)}$ being larger than $V_{P,W}^{(ex)}$.

3. Conclusions

PEG diffusiophoresis occurs from high to low concentration of TMAO (positive diffusiophoresis) in water (see Figure 2). This is consistent with PEG preferential hydration in the presence of TMAO as determined from TMAO osmotic diffusion data (see Figure 1). In other words, PEG migrates in the direction that lowers its chemical potential as expected. If urea replaces TMAO, PEG diffusiophoresis remains positive, although its magnitude is relatively small compared to the TMAO case (see Figure 2). However, urea osmotic diffusion data show that PEG preferentially binds urea (see Figure 1). This implies that PEG migrates in the direction that increases its chemical potential in the presence of urea gradients. A ligand-binding model was, therefore, developed in order to describe positive PEG diffusiophoresis coefficients in the presence of urea in water. This model shows that polymer–cosolute binding is predicted to cause polymer diffusiophoresis from a low to high urea concentration (negative diffusiophoresis). However, its contribution to over-

all polymer diffusiophoresis is also predicted to be relatively small compared to that of polymer–cosolute non-binding interactions. The observed PEG diffusiophoresis from high to low urea concentration (positive diffusiophoresis) is attributed to repulsive hard-core exclusion interactions.

Funding: This research was funded by Texas Christian University RCAF grant number 61008.

Data Availability Statement: Data sharing not applicable. No new data were created or analyzed in this study.

Acknowledgments: We thank Texas Christian University for financial support.

Conflicts of Interest: The authors declare no conflict of interest.

References

1. Bekdemir, A.; Stellacci, F. A centrifugation-based physicochemical characterization method for the interaction between proteins and nanoparticles. *Nat. Commun.* **2016**, *7*, 13121. [CrossRef] [PubMed]
2. Keurentjes, J.T.F.; Janssen, A.E.M.; Broek, A.P.; Van der Padt, A.; Wesselingh, J.A.; Van 'T Riet, K. Multicomponent diffusion in dialysis membranes. *Chem. Eng. Sci.* **1992**, *47*, 1963–1971. [CrossRef]
3. Zhang, J.; Wang, Y.; Wong, T.I.; Liu, X.; Zhou, X.; Liedberg, B. Electrofocusing-enhanced localized surface plasmon resonance biosensors. *Nanoscale* **2015**, *7*, 17244–17248. [CrossRef] [PubMed]
4. Chayen, N.E.; Saridakis, E. Protein crystallization: From purified protein to diffraction-quality crystal. *Nat. Methods* **2008**, *5*, 147–153. [CrossRef] [PubMed]
5. Dey, K.K.; Das, S.; Poyton, M.F.; Sengupta, S.; Butler, P.J.; Cremer, P.S.; Sen, A. Chemotactic separation of enzymes. *ACS Nano* **2014**, *8*, 11941–11949. [CrossRef]
6. Sochacki, K.A.; Shkel, I.A.; Record, M.T.; Weisshaar, J.C. Protein diffusion in the periplasm of *E. coli* under osmotic stress. *Biophys. J.* **2011**, *100*, 22–31. [CrossRef] [PubMed]
7. Vagias, A.; Sergelen, K.; Koynov, K.; Košovan, P.; Dostalek, J.; Jonas, U.; Knoll, W.; Fytas, G. Diffusion and Permeation of Labeled IgG in Grafted Hydrogels. *Macromolecules* **2017**, *50*, 4770–4779. [CrossRef]
8. Kar, A.; Chiang, T.Y.; Rivera, I.O.; Sen, A.; Velegol, D. Enhanced Transport into and out of Dead-End Pores. *ACS Nano* **2015**, *9*, 746–753. [CrossRef]
9. Wesselingh, J.A. Controlling diffusion. *J. Control Release* **1993**, *24*, 47–60. [CrossRef]
10. Miguez, D.G.; Vanag, V.K.; Epstein, I.R. Fronts and pulses in an enzymatic reaction catalyzed by glucose oxidase. *Proc. Natl. Acad. Sci. USA* **2007**, *104*, 6992–6997. [CrossRef]
11. Semenov, S.N.; Markvoort, A.J.; de Greef, T.F.A.; Huck, W.T.S. Threshold Sensing through a Synthetic Enzymatic Reaction-Diffusion Network. *Angew. Chem.-Int. Edit.* **2014**, *53*, 8066–8069. [CrossRef] [PubMed]
12. Velegol, D.; Garg, A.; Guha, R.; Kar, A.; Kumar, M. Origins of concentration gradients for diffusiophoresis. *Soft Matter* **2016**, *12*, 4686–4703. [CrossRef]
13. Shim, S. Diffusiophoresis, Diffusioosmosis, and Microfluidics: Surface-Flow-Driven Phenomena in the Presence of Flow. *Chem. Rev.* **2022**, *122*, 6986–7009. [CrossRef] [PubMed]
14. Anderson, J.L. Colloid Transport by Interfacial Forces. *Annu. Rev. Fluid Mech.* **1989**, *21*, 61–99. [CrossRef]
15. Prieve, D.C. Migration of a colloidal particle in a gradient of electrolyte concentration. *Adv. Colloid Interface Sci.* **1982**, *16*, 321–335. [CrossRef]
16. Peter, Q.A.E.; Jacquat, R.P.B.; Herling, T.W.; Challa, P.K.; Kartanas, T.; Knowles, T.P.J. Microscale Diffusiophoresis of Proteins. *J. Phys. Chem. B* **2022**, *126*, 8913–8920. [CrossRef]
17. Abecassis, B.; Cottin-Bizonne, C.; Ybert, C.; Ajdari, A.; Bocquet, L. Boosting migration of large particles by solute contrasts. *Nat. Mater.* **2008**, *7*, 785–789. [CrossRef] [PubMed]
18. Prieve, D.C.; Roman, R. Diffusiophoresis of a rigid sphere through a viscous electrolyte solution. *J. Chem. Soc. Faraday Trans. 2* **1987**, *83*, 1287–1306. [CrossRef]
19. Guha, R.; Shang, X.; Zydney, A.L.; Velegol, D.; Kumar, M. Diffusiophoresis contributes significantly to colloidal fouling in low salinity reverse osmosis systems. *J. Membr. Sci.* **2015**, *479*, 67–76. [CrossRef]
20. Shin, S.; Shardt, O.; Warren, P.B.; Stone, H.A. Membraneless water filtration using CO_2. *Nat. Commun.* **2017**, *8*, 15181. [CrossRef]
21. Barrios, E.C.; Krause, T.C.; Annunziata, O. Salt-induced diffusiophoresis of a nonionic micelle: Roles of salting out and proximity to surfactant cloud point. *J. Mol. Liq.* **2022**, *359*, 119271. [CrossRef]
22. Lechlitner, L.R.; Annunziata, O. Macromolecule Diffusiophoresis Induced by Concentration Gradients of Aqueous Osmolytes. *Langmuir* **2018**, *34*, 9525–9531. [CrossRef] [PubMed]
23. McAfee, M.S.; Zhang, H.; Annunziata, O. Amplification of salt-induced polymer diffusiophoresis by increasing salting-out strength. *Langmuir* **2014**, *30*, 12210–12219. [CrossRef] [PubMed]
24. Kadajji, V.G.; Betageri, G.V. Water Soluble Polymers for Pharmaceutical Applications. *Polymers* **2011**, *3*, 1972–2009. [CrossRef]

25. Liu, Z.; Robinson, J.T.; Sun, X.M.; Dai, H.J. PEGylated nanographene oxide for delivery of water-insoluble cancer drugs. *J. Am. Chem. Soc.* **2008**, *130*, 10876–10877. [CrossRef]
26. Doane, T.L.; Cheng, Y.; Babar, A.; Hill, R.J.; Burda, C. Electrophoretic Mobilities of PEGylated Gold NPs. *J. Am. Chem. Soc.* **2010**, *132*, 15624–15631. [CrossRef]
27. Kolate, A.; Baradia, D.; Patil, S.; Vhora, I.; Kore, G.; Misra, A. PEG—A versatile conjugating ligand for drugs and drug delivery systems. *J. Control Release* **2014**, *192*, 67–81. [CrossRef]
28. Patist, A.; Kanicky, J.R.; Shukla, P.K.; Shah, D.O. Importance of micellar kinetics in relation to technological processes. *J. Colloid Interface Sci.* **2002**, *245*, 1–15. [CrossRef]
29. Kulkarni, J.A.; Thomson, S.B.; Zaifman, J.; Leung, J.; Wagner, P.K.; Hill, A.; Tam, Y.Y.C.; Cullis, P.R.; Petkau, T.L.; Leavitt, B.R. Spontaneous, solvent-free entrapment of siRNA within lipid nanoparticles. *Nanoscale* **2020**, *12*, 23959–23966. [CrossRef]
30. Uchegbu, I.F.; Vyas, S.P. Non-ionic surfactant based vesicles (niosomes) in drug delivery. *Int. J. Pharm.* **1998**, *172*, 33–70. [CrossRef]
31. Record, M.T.; Anderson, C.F. Interpretation of preferential interaction coefficients of nonelectrolytes and of electrolyte ions in terms of a two-domain model. *Biophys. J.* **1995**, *68*, 786–794. [CrossRef] [PubMed]
32. Timasheff, S.N. Protein-solvent preferential interactions, protein hydration, and the modulation of biochemical reactions by solvent components. *Proc. Natl. Acad. Sci. USA* **2002**, *99*, 9721–9726. [CrossRef] [PubMed]
33. Schurr, J.M.; Rangel, D.P.; Aragon, S.R. A contribution to the theory of preferential interaction coefficients. *Biophys. J.* **2005**, *89*, 2258–2276. [CrossRef] [PubMed]
34. Barrios, E.C.; Penino, K.V.; Annunziata, O. Diffusiophoresis of a Nonionic Micelle in Salt Gradients; Roles of Preferential Hydration and Salt-Induced Surfactant Aggregation. *Int. J. Mol. Sci.* **2022**, *23*, 13710. [CrossRef] [PubMed]
35. Annunziata, O.; Buzatu, D.; Albright, J.G. Protein diffusiophoresis and salt osmotic diffusion in aqueous solutions. *J. Phys. Chem. B* **2012**, *116*, 12694–12705. [CrossRef]
36. Annunziata, O.; Fahim, A. A unified description of macroion diffusiophoresis, salt osmotic diffusion and collective diffusion coefficient. *Int. J. Heat Mass Transf.* **2020**, *163*, 120436. [CrossRef]
37. Vergara, A.; Capuano, F.; Paduano, L.; Sartorio, R. Lysozyme Mutual Diffusion in Solutions Crowded by Poly(ethylene glycol). *Macromolecules* **2006**, *39*, 4500–4506. [CrossRef]
38. Annunziata, O. On the role of solute solvation and excluded-volume interactions in coupled diffusion. *J. Phys. Chem. B* **2008**, *112*, 11968–11975. [CrossRef]
39. McAfee, M.S.; Annunziata, O. Effects of Salting-In Interactions on Macromolecule Diffusiophoresis and Salt Osmotic Diffusion. *Langmuir* **2015**, *31*, 1353–1361. [CrossRef]
40. Fahim, A.; Annunziata, O. Amplification of Salt-Induced Protein Diffusiophoresis by Varying Salt from Potassium to Sodium to Magnesium Chloride in Water. *Langmuir* **2020**, *36*, 2635–2643. [CrossRef]
41. Anderson, C.F.; Courtenay, E.S.; Record, M.T. Thermodynamic Expressions Relating Different Types of Preferential Interaction Coefficients in Solutions Containing Two Solute Components. *J. Phys. Chem. B* **2002**, *106*, 418–433. [CrossRef]
42. Zhang, H.X.; Annunziata, O. Macromolecular hydration compared with preferential hydration and their role on macromolecule-osmolyte coupled diffusion. *Phys. Chem. Chem. Phys.* **2009**, *11*, 8923–8932. [CrossRef] [PubMed]
43. Arakawa, T.; Timasheff, S.N. Preferential interactions of proteins with salts in concentrated solutions. *Biochemistry* **1982**, *21*, 6545–6552. [CrossRef]
44. van Holde, K.E.; Johnson, W.C.; Ho, P.S. *Principles of Physical Biochemistry*, 2nd ed.; Pearson, Prentice Hall: Hoboken, NJ, USA, 2006.
45. Miller, D.G. Thermodynamics of irreversible processes—The experimental verification of the onsager reciprocal relations. *Chem. Rev.* **1960**, *60*, 15–37. [CrossRef]
46. Onsager, L. Reciprocal Relations in Irreversible Processes. I. *Phys. Rev.* **1931**, *37*, 405–426. [CrossRef]
47. Ribeiro, A.C.F.; Musilova, L.; Mracek, A.; Cabral, A.; Santos, M.A.; Cabral, I.; Esteso, M.A.; Valente, A.J.M.; Leaist, D. Host-guest paracetamol/cyclodextrin complex formation evaluated from coupled diffusion measurements. *J. Chem. Thermodyn.* **2021**, *161*, 106551. [CrossRef]
48. Paduano, L.; Sartorio, R.; Vitagliano, V.; Costantino, L. Diffusion coefficients of the system alpha-cyclodextrin-n-butylurea-water at 25 degrees C. *J. Solut. Chem.* **1995**, *24*, 1143–1153. [CrossRef]